



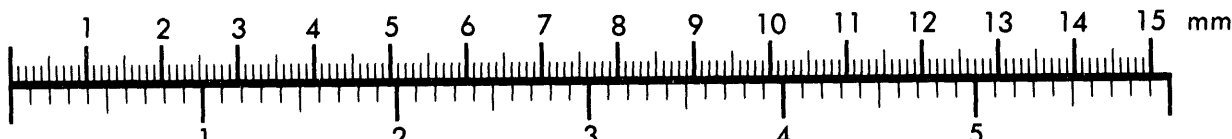
AIM

Association for Information and Image Management

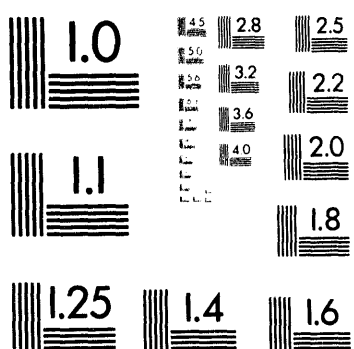
1100 Wayne Avenue, Suite 1100
Silver Spring, Maryland 20910

301/587-8202

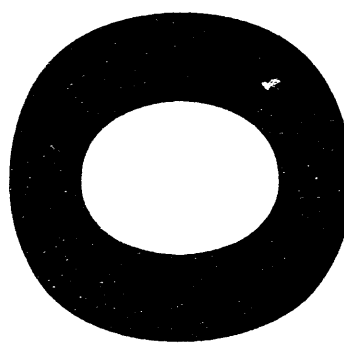
Centimeter



Inches



MANUFACTURED TO AIIM STANDARDS
BY APPLIED IMAGE, INC.



Conf-940874--2

LA-UR- 94-1073

Title:

Substitutional Effects on the Electronic Transport
of the Kondo Insulator $\text{Ce}_3\text{Bi}_4\text{Pt}_3$

Author(s):

M.F. Hundley
J.D. Thompson
Z. Fisk
P.C. Canfield

Submitted to:

6th Joint MMM-Intermag Conference
Albuquerque, NM
10 August 1994

DISCLAIMER

This report was prepared as an account of work sponsored by an agency of the United States Government. Neither the United States Government nor any agency thereof, nor any of their employees, makes any warranty, express or implied, or assumes any legal liability or responsibility for the accuracy, completeness, or usefulness of any information, apparatus, product, or process disclosed, or represents that its use would not infringe privately owned rights. Reference herein to any specific commercial product, process, or service by trade name, trademark, manufacturer, or otherwise does not necessarily constitute or imply its endorsement, recommendation, or favoring by the United States Government or any agency thereof. The views and opinions of authors expressed herein do not necessarily state or reflect those of the United States Government or any agency thereof.

Los Alamos
NATIONAL LABORATORY

Los Alamos National Laboratory, an affirmative action/equal opportunity employer, is operated by the University of California for the U.S. Department of Energy under contract W-7405-ENG-36. By acceptance of this article, the publisher recognizes that the U.S. Government retains a nonexclusive, royalty-free license to publish or reproduce the published form of this contribution, or to allow others to do so, for U.S. Government purposes. The Los Alamos National Laboratory requests that the publisher identify this article as work performed under the auspices of the U.S. Department of Energy.

DISTRIBUTION OF THIS DOCUMENT IS UNLIMITED

Sc Form No. 836 R5
ST 2629 10/91

Substitutional Effects on the Electronic Transport of the Kondo Insulator $\text{Ce}_3\text{Bi}_4\text{Pt}_3$

M.F. Hundley, P.C. Canfield,[†] J.D. Thompson, and Z. Fisk

Los Alamos National Laboratory, Los Alamos, NM 87545 USA

Abstract

The resistivity ρ and thermoelectric power S of the doped Kondo insulator $(\text{Ce}_{1-x}\text{La}_x)_3\text{Bi}_4\text{Pt}_3$ are examined to determine the effects of doping on the narrow gap exhibited by this compound. With increasing La concentration the energy gap progressively disappears in both ρ and S and band-like transport develops below 25 K. The $T=0$ transport energy gap as determined from either ρ or S scales with the single-impurity Kondo energy scale T_K as determined from magnetic susceptibility measurements, independently of x for $x \leq 0.25$. This result strongly suggests that the gap arises from band hybridization that is driven by Kondo-like many-body correlations rather than from single-electronic interactions.

PACS: 75.20.Hr, 71.28.+d, 72.20.-I

Submitted to the 6th joint MMM-Intermag Conference

A number of well-known ground states occur in f-electronic systems that result from the competition between electronic and magnetic correlations; these ground states include the heavy fermion or mixed-valent states, unconventional superconductivity, and antiferromagnetic order.¹ Recently, a new ground states referred to as a Kondo insulator has been identified.² These systems exhibit extremely narrow energy gaps E_g on the order of 100 K as determined from both electronic transport³ and inelastic neutron scattering measurements.⁴ Lattice constant measurements show an anomalous thermal expansion coefficient and a Gruneisen parameter $\Omega \approx 36$ indicative of mixed-valent behavior.⁵ A straightforward interpretation of the behavior exhibited by a Kondo insulator is that the energy gap is derived from hybridization between a wide conduction band and an f-band that is renormalized to the Fermi level via Kondo-like many-body interactions. An indirect gap results if the electron count is precisely two per unit cell, totally filling the valence band. Mean-field treatments^{6,7} of the Anderson lattice Hamiltonian suggest that the energy gap should scale with the single-impurity Kondo energy scale T_K and that the gap should be a decreasing function of temperature; transport measurements⁸ on the Kondo insulator $\text{Ce}_3\text{Bi}_4\text{Pt}_3$ indicate that, as predicted, the energy gap is strongly temperature-dependent.

If the narrow energy gap in Kondo insulators is a manifestation of many-body interactions then the gap should be strongly affected by non-magnetic substitution for the f-element. Further, the quantitative effect of f-moment substitution should be quite different from that expected for a gap resulting from conventional single-electron physics. A theoretical model⁹ of non-magnetic doping effects on Kondo insulators based on an Anderson lattice Hamiltonian suggests that the non-magnetic impurities form Kondo holes that break the translational invariance, and, in turn, the coherence of the ground state. With finite concentrations of Kondo holes an impurity band forms

inside the gap. Below a critical doping level, the energy gap persists and the impurity band acts in parallel with the semiconducting valence and conduction bands.

To determine the importance of f-moment periodicity on the energy gap in Kondo insulators we performed an electronic transport study on the effects of non-magnetic La substitution for Ce in the Kondo insulator $\text{Ce}_3\text{Bi}_4\text{Pt}_3$. This compound exhibits a narrow energy gap E_g ($T \rightarrow 0$) ≈ 130 K in electrical resistivity ρ , thermoelectric power (TEP) S , and Hall constant R_H ,¹⁰ the gap is also reflected in the magnetic susceptibility. We have measured the resistivity and thermoelectric power of $(\text{Ce}_{1-x}\text{La}_x)_3\text{Bi}_4\text{Pt}_3$ for six dopant levels ($x = 0, 0.01, 0.1, 0.25, 0.5, 1.0$) from 4 K to 325 K. With increasing La concentration the gap progressively disappears in both ρ and S and band-like transport develops below 25 K. Further, the energy gap is found to scale with the characteristic Kondo energy scale T_K as inferred from magnetic susceptibility measurements for $x \leq 0.25$. This suggests that the energy gap forms from band hybridization that is driven by many-body, rather than single-electron, interactions.

Single crystals of $(\text{Ce}_{1-x}\text{La}_x)_3\text{Bi}_4\text{Pt}_3$ were grown from a bismuth flux with nominal lanthanum concentrations of $x = 0, 0.01, 0.1, 0.25, 0.5$, and 1.0. For each doping concentration ρ and S measurements were performed on the same specimen. A conventional four-probe dc technique was employed in measuring the resistivity, while the TEP was measured by suspending a single crystal between two electrically isolated copper posts across which a variable temperature gradient was applied; electrical contacts were made using a silver conductive paint.

The normalized resistivity of La-doped $\text{Ce}_3\text{Bi}_4\text{Pt}_3$ is depicted in Fig. 1. ρ for pure $\text{Ce}_3\text{Bi}_4\text{Pt}_3$ shows a rapid rise with decreasing temperature indicative of activated behavior. At room temperature the resistivity of $\text{Ce}_3\text{Bi}_4\text{Pt}_3$ ($\rho(300$ K) ≈ 200 $\mu\Omega$ cm) is typical of a mixed-

valent compound in the single-impurity Kondo regime. A detailed analysis⁸ of $\rho(T)$ involving degenerate semiconductor statistics (valid for $E_g \approx k_B T$) indicates that $E_g(100 \text{ K}) = 90 \text{ K}$ and that the gap decreases with increasing temperature. Below 50 K extrinsic effects (i.e. impurities) dominate the resistivity. As Ce is replaced by La the resistivity drops markedly; with just 1% La, ρ drops by a factor of 50 at 4 K relative to the undoped material. Out to 50% doping, dR/dT continues to be negative. Pure $\text{La}_3\text{Bi}_4\text{Pt}_3$ has a resistivity indicative of a dirty metal with a short mean-free path.¹¹ At 1% La doping the resistivity exhibits a maximum near 25 K below which ρ approaches a T^2 temperature dependence suggestive of Fermi-liquid like behavior. With 10% La doping a local peak in ρ is also evident near 25 K.

The TEP of La-doped $\text{Ce}_3\text{Bi}_4\text{Pt}_3$ is presented in Fig. 2. For the undoped material S rises with decreasing temperature, reaches a maximum at 20 K and drops with decreasing temperature. Above 80 K the TEP exhibits semiconducting behavior ($S \propto 1/T$); an analysis involving degenerate electron statistics⁸ indicates that $E_g(100 \text{ K}) = 95 \text{ K}$, and that the gap falls with increasing temperature. As with ρ and R_H ,¹⁰ the TEP below 80 K is characteristic of transport dominated by an extrinsic conduction mechanism as is common in impure semiconductors. When doped with 1% La, S rises to a larger value than for pure $\text{Ce}_3\text{Bi}_4\text{Pt}_3$. A detailed energy gap analysis (see below) indicates that the gap is essentially the same for pure and 1% doped $\text{Ce}_3\text{Bi}_4\text{Pt}_3$. Hence, the enhanced peak for $(\text{Ce}_{0.99}\text{La}_{0.01})_3\text{Bi}_4\text{Pt}_3$ may be a growth artifact which reflects a reduction in the extrinsic conduction mechanism upon very light La doping. With increased doping the TEP progressively drops at all temperatures indicative of an increase in carrier concentration and a reduction in the energy gap. For $\text{La}_3\text{Bi}_4\text{Pt}_3$ the TEP is negative at all

temperature with a temperature dependence characteristic of a metal with a low concentration of carriers.

The transport data in Figs. 1 and 2 indicate that moderate alloying with La suppresses the energy gap and gives rise to band-like behavior below 25 K. For 1% and 10% La doping there are indications in ρ that a partially coherent, Fermi-liquid like regime is approached (i.e., $d\rho/dT > 0$) below 25 K. These results are consistent with the semiconducting behavior exhibited in $\text{Ce}_3\text{Bi}_4\text{Pt}_3$ arising from band hybridization involving a renormalized f-band. Alloying with La acts to disrupt the f-moment lattice periodicity which in turn suppresses the energy gap by inhibiting the many-body interactions responsible for the band renormalization.

To move towards a more quantitative analysis we will examine the transport data in terms of a Kondo-hole impurity model.⁹ In this model a $(1/d)$ expansion is employed to determine the effects of non-magnetic doping on a Kondo insulator. The non-magnetic dopant forms a Kondo-hole impurity band which resided inside the energy gap. The band has both a height and width proportional to $x^{1/2}$. The impurity doping does not directly change the Kondo energy scale T_K . The gap energy is similarly unaffected for doping below the critical threshold where the impurity bandwidth reaches and exceeds E_g . Experimental support for this model is provided by specific heat measurements¹² on La doped $\text{Ce}_3\text{Bi}_4\text{Pt}_3$ which indicate that the T-linear contribution to C_p does grow as $x^{1/2}$.

In analyzing the ρ and TEP data we assume that the Kondo-hole impurity band which acts in parallel with the semiconducting bands has the characteristics of a dirty, poorly conducting metal. The transport properties of the system will then be determined by the better conducting valence and conduction bands. As such, both ρ and S should display semiconducting behavior. A

quantitative analysis must employ degenerate semiconductor electron statistics^{8,13} since $\text{Ce}_3\text{Bi}_4\text{Pt}_3$ is not in the degenerate ($E_g \gg k_B T$) limit. The system is modeled as two wide parabolic bands separated by $E_g(T)$. This is a reasonable assumption for the upper and lower hybridization bands away from the Brillouin zone edge; the f-like states near the band edges will have a very low mobility, and, as such, will not contribute significantly to the transport. In addition, we assume that scattering is dominated by electron-phonon interactions.⁸ Expressions for the resistivity and TEP valid for $E_g \approx k_B T$ are given by

$$\rho(T) = \rho_0 / \ln \left\{ 1 + \exp(-E_g / k_B T) \right\} \quad , \quad (1)$$

$$S = \frac{-k_B}{e} \left\{ \frac{2F_1(-E_g / k_B T)}{F_0(-E_g / k_B T)} + \frac{E_g}{k_B T} \right\} \quad , \quad (2)$$

where ρ_0 is a constant, k_B is the Boltzmann constant, e is the electron's charge, and $F_n(x)$ is the nth-order Fermi-Dirac integral

$$F_n(x) = \int_0^{\infty} \frac{\varepsilon^n}{1 + \exp(\varepsilon - x)} d\varepsilon \quad . \quad (3)$$

$E_g(T)$ can be determined by employing Eqns. 1-3 in tandem with the transport data in Figs. 1 and 2 to compose a self-consistent numerical calculation. The results of this analysis are presented in Fig. 3 where $E_g(100 \text{ K})$ as determined from both ρ and S data is plotted as a function of La concentration. $E_g(100 \text{ K})$ drops from 95 K (8.2 meV) for pure $\text{Ce}_3\text{Bi}_4\text{Pt}_3$ to 40 K (3.4 meV) for $x=0.25$, and 15 K (1.3 meV) for $x=0.5$.

If the narrow energy gap evident in both pure and La doped $\text{Ce}_3\text{Bi}_4\text{Pt}_3$ is a manifestation of band hybridization driven by many-body renormalization then the magnitude of the gap should scale with the characteristic single-impurity Kondo energy scale T_K . This energy can be

determined from the temperature T_{\max} where a maximum occurs in the dc magnetic susceptibility χ ; a Bethe-ansatz theory valid for $J=5/2$ Ce indicates that $T_K = 4 T_{\max}$.¹⁴ $T_{\max}(x)$ was previously reported¹² and the results appear as open triangles in Fig. 3. T_{\max} and hence T_K decrease with increasing La concentration. This would appear to be at odds with the Kondo-hole impurity model wherein E_g is independent of x (in that model the gap energy is dominated by Coulomb repulsion which should be weakly dependent on x). This discrepancy is lifted when the effect of La doping on the lattice constant, coupled with the large Gruneisen parameter for $\text{Ce}_3\text{Bi}_4\text{Pt}_3$, is considered. The lattice constant for $\text{La}_3\text{Bi}_4\text{Pt}_3$ is 1% larger than for $\text{Ce}_3\text{Bi}_4\text{Pt}_3$ at 4 K.⁵ Hence, with progressively increasing La doping the lattice expands under an negative effective chemical pressure. Just as hydrostatic pressure enhances the mixed-valent nature of $\text{Ce}_3\text{Bi}_4\text{Pt}_3$ and increases the gap,¹² increased La doping expands the lattice, favoring the smaller tri-valent 4f over the tetra-valent 4f⁰ configuration. This reduces the mixed-valence of the compound which then reduces the hybridization, T_K , and the energy gap.

The T_{\max} and $E_g(100 \text{ K})$ data in Fig. 3 indicate that both quantities decrease with increasing La concentration. The renormalized f-band description of a Kondo insulator indicates that the energy gap should itself be a decreasing function of temperature, $E_g(T) = f(T/T_K)$.^{6,7} Hence, to quantitatively compare the transport energy scale E_g and the Kondo energy scale T_K we must renormalize $E_g(100 \text{ K})$ to $E_g(T = 0)$. Measurements on pure $\text{Ce}_3\text{Bi}_4\text{Pt}_3$ indicate that the mean-field prediction in Ref. 7 provides a good description of $f(T/T_K)$. By employing this function, $E_g(0)$ can be determined from $E_g(100 \text{ K})$ and T_K . The ratio $E_g(0)/T_K$ with $T_K \equiv 4 T_{\max}$ is plotted as a function of La concentration in Fig. 3 (open squares). For $x=0$ to 0.25 this ratio is independent of x to within 10 %. Given the large uncertainties involved in the estimate of

$E_g(0)/T_K$, it appears that for low to moderate levels of La doping concentrations *the transport energy gap tracks the Kondo energy scale*. Only with 50 % doping is there considerable deviation in the ratio; with $x = 0.5$ many of the assumptions involved in the analysis may be invalid. As such, it is not surprising that when one-half of the f-moments are replaced the transport and Kondo energies are no longer coupled. Hence, at up to moderate doping levels a single energy, the single-impurity Kondo energy T_K , can describe the magnetic, thermodynamic, and transport properties of Kondo insulators. This lends support to the description wherein many-body interactions control the properties exhibited by these systems.

An alternative to this description of the Kondo insulator is that many-body effects play no part in the underlying physics. In this framework $\text{Ce}_3\text{Bi}_4\text{Pt}_3$ is a conventional narrow-band semiconductor wherein La doping produces a metallic impurity band which suppresses the activated transport properties. A description of this type is intractable because it cannot explain the large linear contribution to C_p that develops with La doping. Similarly, this conventional description would not predict that the transport gap energy would scale with T_{\max} as a function of La doping. Hence, it seems unlikely that a conventional (i.e., single-electron) semiconductor model of Kondo insulators can explain the magnetic, transport, and thermodynamic behavior exhibited by the system $(\text{Ce}_{1-x}\text{La}_x)_3\text{Bi}_4\text{Pt}_3$ while many-body renormalization models predict this behavior explicitly.

In summary, a careful study of the transport properties of $(\text{Ce}_{1-x}\text{La}_x)_3\text{Bi}_4\text{Pt}_3$ indicates that La substitution acts to progressively decrease E_g with increasing x . The decrease in $E_g(0)$ with increasing x tracks a similar decrease in the single-impurity Kondo energy T_K . A single energy scale, T_K , can therefore describe the transport (ρ and S), magnetic (χ), and thermodynamic (C_p)

properties of the Kondo insulator $\text{Ce}_3\text{Bi}_4\text{Pt}_3$. This suggests strongly that the semiconducting properties exhibited by Kondo insulators arise from band hybridization between a conventional conduction band and a renormalized f-band wherein the renormalization is driven by Kondo-like many-body correlations rather than by single-electron interactions.

Acknowledgments

We thank J. Lawrence and D. Mandrus for useful discussions. This work was performed under the auspices of the U.S. Department of Energy.

References

¹ Present address: Ames Laboratory, Iowa State University, Ames, Iowa 50011, USA.

² For a review see: N. Grewe and F. Steglich, *Handbook of Physics and Chemistry of Rare Earths*, Vol. 14. K.A. Gschmidner and L. Eyring, eds. (Elsevier , 1991).

³ G. Aeppli and Z. Fisk, *Comments Cond. Mat. Phys.* **16**, 155 (1992).

⁴ M.F. Hundley, P.C. Canfield, J.D. Thompson, Z. Fisk, and J.M. Lawrence, *Phys. Rev. B* **42**, 6842 (1990).

⁵ A. Severing, J.D. Thompson, P.C. Canfield, Z. Fisk, and P.S. Riseborough, *Phys. Rev. B* **44**, 6832 (1991).

⁶ G. H. Kwei, J.M. Lawrence, P.C. Canfield, W.P. Beyermann, J.D. Thompson, Z. Fisk, A.C. Lawson, and J.S. Goldstone, *Phys. Rev. B* **46**, 8067 (1992).

⁷ P.S. Riseborough, *Phys. Rev. B* **45**, 13984 (1992).

⁸ C. Sanchez-Castro, K.S. Bedell, and B.R. Cooper, *Phys. Rev. B* **47**, 6879 (1993).

⁹ M.F. Hundley, P.C. Canfield, J.D. Thompson, and Z. Fisk, *Physica B* (in press).

¹⁰ P. Schlottmann, *Phys. Rev. B* **46**, 998 (1992).

¹¹ M.F. Hundley, P.C. Canfield, J.D. Thompson, Z. Fisk, and J.M. Lawrence, *Physica B* **171**, 254 (1991).

¹² M.F. Hundley, A. Lacerda, P.C. Canfield, J.D. Thompson, and Z. Fisk, *Physica B* **186-188**, 425 (1993).

¹³ J.D. Thompson, W.P. Beyermann, P.C. Canfield, Z. Fisk, M.F. Hundley, G.H. Kwei, R.S. Kwok, A. Lacerda, J.M. Lawrence, and A. Severing, *Transport and Thermal Properties of f-Electron Systems*, eds. H. Fujii, T. Fujita, and G. Oomi (Plenum, NY 1993).

¹³ D.R. Lovett, *Semimetals & Narrow-band Gap Semiconductors* (Pion, London 1977).

¹⁴ V.T. Rajan, *Phys. Rev. Lett.* **51**, 308 (1983).

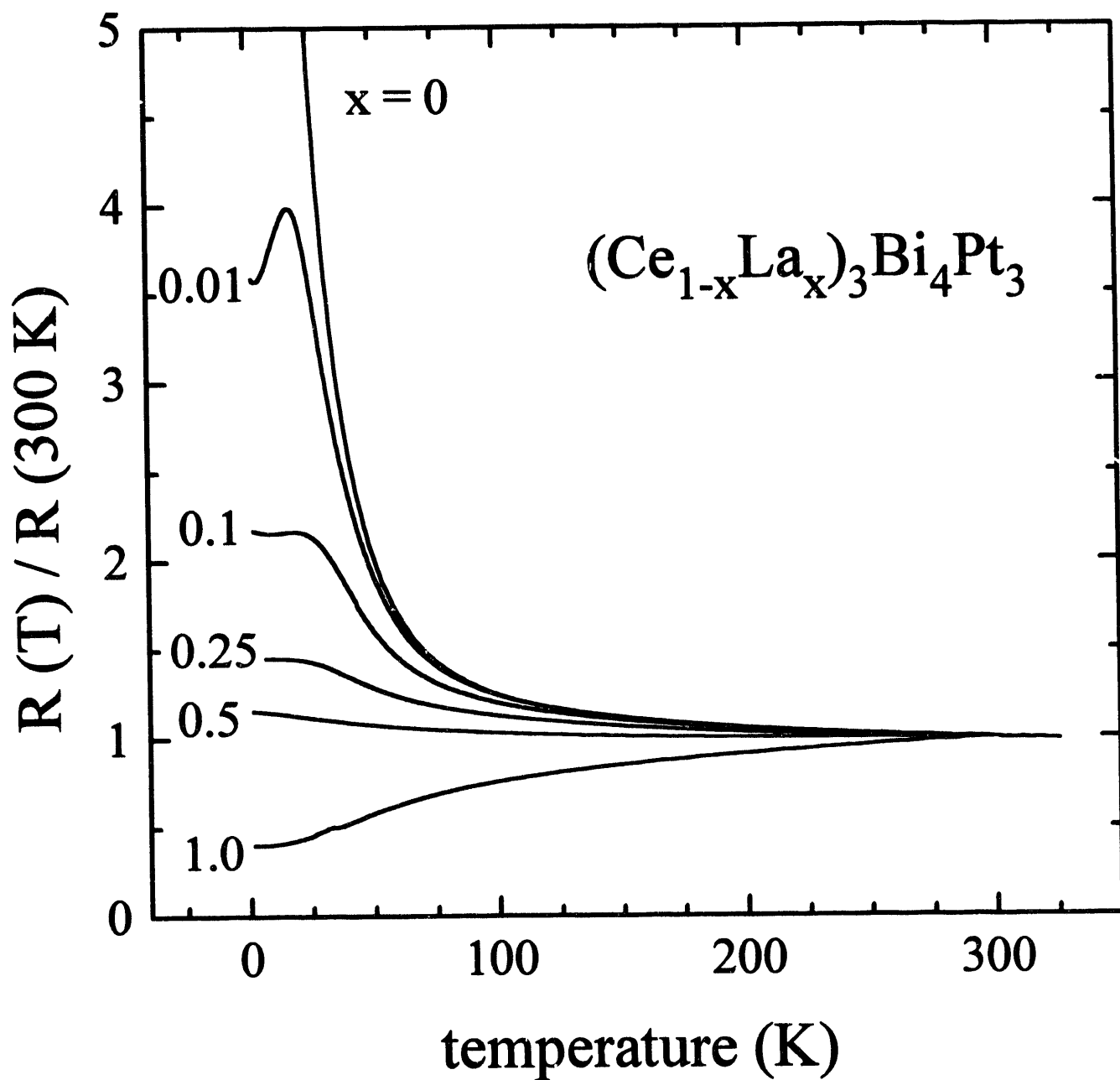
Figure Captions

Fig. 1: ρ normalized at 300 K plotted versus T for six La doping concentrations.

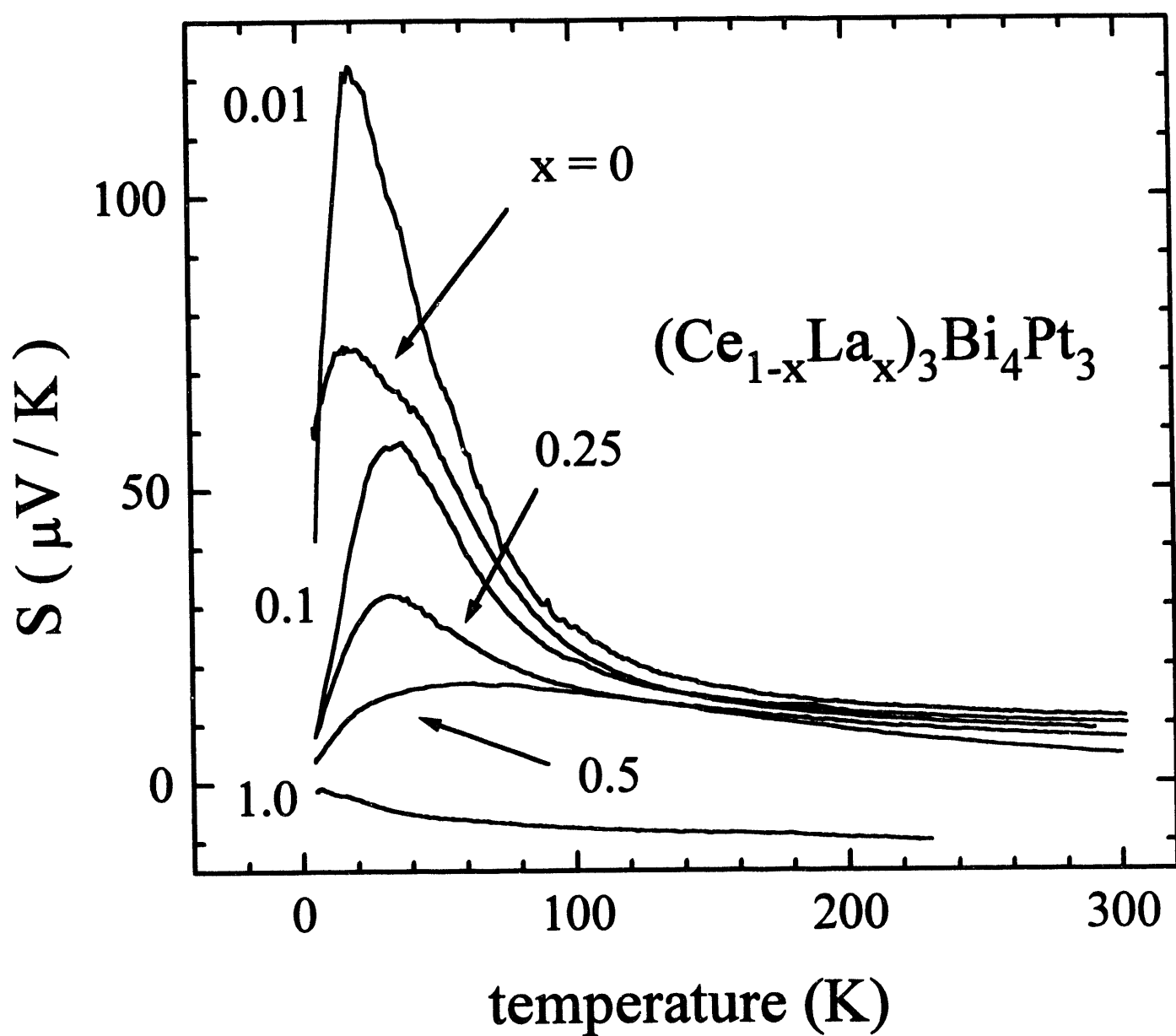
Fig. 2: The TEP plotted versus temperature for six La doping concentrations.

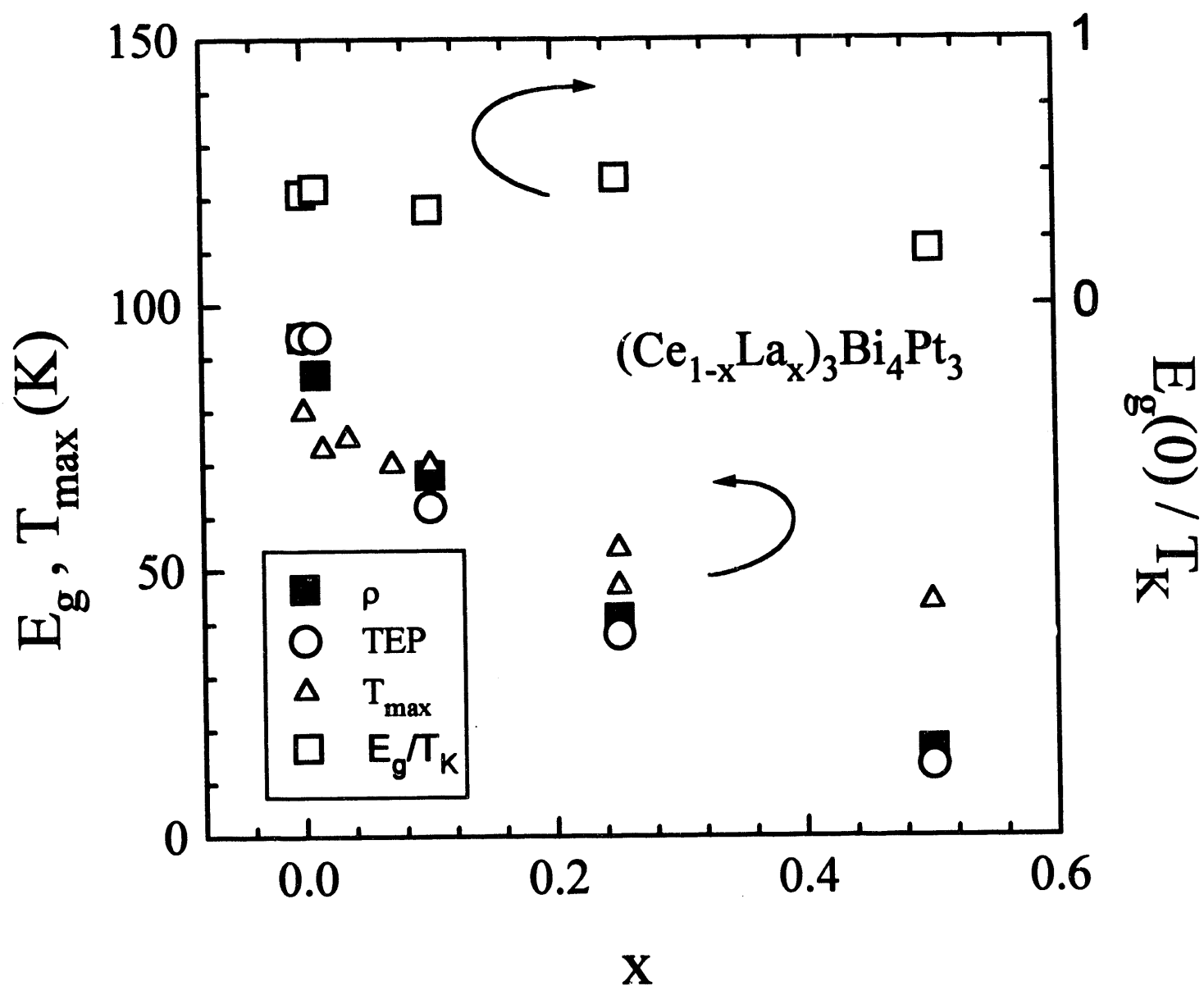
Fig. 3: Transport energy gap E_g at 100 K, T_{max} , and $E_g(T=0)/T_K$ plotted versus La concentration

\times $E_g(T=0)/T_K$ data (open squares) are plotted on the right axis while the transport gaps inferred from resistivity (solid squares) and thermoelectric power (open circles) data are plotted on the left axis. T_{max} is also plotted on the left axis.



Hundley, *et al.* Fig. 1

Hundley, *et al.* Fig. 2

Hundley, *et al.* Fig. 3

DATE
FILMED

7/7/94

END

